JOURNAL OF VIROLOGY, June 2006, p. 5897–5907 Vol. 80, No. 12
0022-538X/06/$08.00+0 doi:10.1128/JVI.00008-06


# Identification of an N-Terminal Trimeric Coiled-Coil Core within Arenavirus Glycoprotein 2 Permits Assignment to Class I Viral Fusion Proteins

Bruno Eschli,[1]* Katharina Quirin,[2] Alexander Wepf,[1] Jacqueline Weber,[1] Rolf Zinkernagel,[1] and Hans Hengartner[1]

*Institute of Experimental Immunology, University Hospital Zürich, Schmelzbergstrasse 12, CH-8091 Zürich, Switzerland,[1] and Institute of Biochemistry, Swiss Federal Institute of Technology, ETH Hoenggerberg, CH-8093 Zürich, Switzerland[2]*

Received 3 January 2006/Accepted 28 March 2006

**The lymphocytic choriomeningitis virus (LCMV) glycoprotein (GP) consists of the transmembrane subunit GP-2 and the receptor binding subunit GP-1. Both are synthesized as one precursor protein and stay noncovalently attached after cleavage. In this study, we determined the oligomeric state of the LCMV GP and expressed it in two different conformations suitable for structural analysis. Sequence analysis of GP-2 identified a trimeric heptad repeat pattern containing an N-terminal α-helix. An α-helical peptide matching this region formed a stable oligomer as revealed by gel filtration chromatography and dynamic light scattering. In contrast, a second α-helical peptide corresponding to a predicted C-terminal α-helix within GP-2 did not oligomerize. Refolding of the complete GP-2 ectodomain revealed trimeric all-alpha complexes probably representing the six-helix bundle state that is considered a hallmark of class I viral fusion proteins. Based on these results, we generated a construct consisting of the complete uncleavable LCMV GP ectodomain fused C-terminally to the trimeric motif of fibritin. Gel filtration analysis of the secreted fusion protein identified two complexes of ~230 and ~440 kDa. Both complexes bound to a set of conformational and linear antibodies. Cross-linking confirmed the 230-kDa complex to be a trimer. The 440-kDa complexes were found to represent disulfide-linked pairs of trimers, since partial reduction converted them to a complex species migrating at 250 kDa. By electron microscopy, the 230-kDa complexes appeared as single spherical particles and showed no signs of rosette formation. Our results clearly demonstrate that the arenavirus GP is a trimer and must be considered a member of the class I viral fusion protein family.**

Arenaviruses are enveloped RNA viruses with a single-stranded bisegmented genome (40). The small RNA segment contains two genes that code for the nucleoprotein (NP) and the glycoprotein precursor (GPC). The large segment codes for the viral polymerase (L protein) and the Z protein. The arenavirus family is divided into the Old World group, including the prototypic family members lymphocytic choriomeningitis virus (LCMV) and Lassa virus, and the New World group, including the Junín, Machupo, Guanarito, and Sabia viruses (5). Lassa, Junín, Machupo, Guanarito, and Sabia viruses are the causes of severe hemorrhagic fevers in western Africa, Argentina, Bolivia, Venezuela, and Brazil, respectively (8). Because they cause high fatality rates in humans, they are a major health issue.

With respect to antiviral strategies, the glycoprotein (GP) spike of enveloped viruses is of special interest, since it mediates two major steps in infection. First, attachment to a specific cellular receptor has to be established and second, membrane fusion must be achieved. Thus, a detailed molecular characterization of the arenavirus GP will enable efforts to inhibit infection by either interfering with the GP receptor interaction or mechanistically blocking viral membrane fusion (24).

Based on their structure-function relationships, viral glycoproteins mediating membrane fusion have been classified to belong to either class I or class II fusion proteins (17, 20, 21, 23, 31, 33, 35, 46, 50). The class I fusion proteins are translated as GP precursor proteins, which are proteolytically processed to give rise to metastable trimers consisting of heterodimers. Whereas the peripheral head subunit mediates receptor binding, the transmembrane subunit is responsible for membrane fusion itself. Based on the hemagglutinin of the orthomyxovirus influenza, which was the first fusion protein to be structurally characterized in both pre- and postfusion conformations, a general model of class I viral membrane fusion was postulated (50). This model states that certain triggers, for example, a low pH in the case of the influenza hemagglutinin, are needed for the initial destabilization of the proteolytically activated trimer. Destabilization sets off a series of conformational rearrangements within the transmembrane subunit leading to the formation of the postfusion six-helix bundle conformation. This state is characterized by C-terminal α-helices packing into the hydrophobic grooves of a trimeric coiled-coil core, formed by N-terminal α-helices. Thereby, the viral envelope and the target membrane are drawn together to give rise to the fusion pore.

The arenavirus GP shares most characteristics of class I fusion proteins. GP is translated as a single precursor protein (GPC) into the lumen of the endoplasmic reticulum, where the 58-amino-acid-long signal peptide is cleaved off (10). After cleavage, the signal peptide stays associated with the GPC and is somehow involved in the further proteolytic processing of

* Corresponding author. Mailing address: Institute of Experimental Immunology, University Hospital Zürich, Schmelzbergstrasse 12, CH-8091 Zürich, Switzerland. Phone: 41 (0) 44 255 2734. Fax: 41 (0) 44 255 4420. E-mail: eschlib@student.ethz.ch.

the GPC in the secretory pathway (25, 26). GPC undergoes extensive N-linked glycosylation (55) and is thought to oligomerize within the endoplasmic reticulum before being proteolytically processed between the medial and the *trans*-Golgi network by the subtilase SKI-1/S1P (3, 38, 55). Proteolysis yields the integral membrane protein GP-2 (35 kDa) and the highly glycosylated peripheral protein GP-1 (44 kDa), which stay noncovalently attached to each other. A recent electron cryomicroscopy study visualized the spikes as single-lobed or double-lobed structures being 9.5 nm in height and either 6.7 nm (single lobed) or 7.9 nm (double lobed) in width (41). A 3-nm-long stalk region, presumably showing the GP-2 subunit and a spherical head region formed by the GP-1 subunit, were clearly distinguishable.

In accordance with the general class I architecture, the arenavirus GP-1 subunit has been shown to mediate receptor binding. Monoclonal LCMV-neutralizing antibodies, which were found to block virus attachment to the cell surface, have been shown to bind to a single site on GP-1 (4, 42). The main receptor for most arenaviruses, including the LCMV-WE strain and Lassa virus, is α-dystroglycan (4, 14, 37, 51). Binding to α-dystroglycan is thought to involve lectin-like recognition of *O*-mannosyl-linked carbohydrates (32, 36). Receptor binding mediates uptake into intracellular compartments, where acid-induced membrane fusion occurs. This event can be inhibited by lysotropic drugs like chloroquine and monesin. Furthermore, low-pH treatment of purified LCMV virions resulted in the release of the GP-1 subunit and in membrane fusion with liposomes (at pH 5.5) (4, 18, 19).

The stoichiometry of the GP spike has been controversial and has thwarted its classification as a class I fusion protein (23, 35). Cross-linking experiments carried out with purified LCMV indicated that the GP-1/GP-2 heterodimers would form tetramers, which were partly disulfide linked among their GP-1 subunits (7, 8, 12). A computational modeling approach, however, uncovered a high degree of similarity between the LCMV GP-2 subunit and other well-characterized trimeric transmembrane subunits, belonging to the retrovirus and the filovirus families (27). It should be noted that initial cross-linking experiments with purified human immunodeficiency virus particles also indicated a tetrameric structure for gp160 (22, 45), and only later on the complexes turned out to be trimers instead.

The aim of this study was to determine the oligomeric state of the LCMV GP spike and to express and purify the ectodomain and fragments of it in a manner suitable for further structural analysis.

## MATERIALS AND METHODS

**Antibodies.** A hybridoma cell line producing KL25 (immunoglobulin G1 [IgG1]) was originally obtained from F. Lehmann-Grube (Heinrich Pette Institut, Hamburg, Germany) (6). Hybridomas producing Wen3 (IgG2a) and Wen4 (IgG2a) were established by this laboratory (47). Ascites fluids of the antibodies WE 18.8 (IgG1) and WE 83.4 (IgG2a) were a generous gift from M. Buchmeier (Scripps Research Institute, La Jolla, California) and have been characterized in a comprehensive epitope-mapping study (9, 42). Detection was carried out using either horseradish peroxidase (HRP)-coupled anti-mouse IgG1 antibody (Zymed, San Francisco, California) or anti-mouse IgG2a antibody (Zymed, San Francisco, California).

**Purification of peptides and dynamic light scattering.** Synthetic lyophilized peptides, matching the helix 1 (peptide 1) and helix 2 (peptide 2) regions, were purchased from Anawa Trading SA, Wangen, Switzerland, at a purity of 96%. Both peptides were resuspended in 10 mM Tris-HCl, pH 7.35, with 130 mM NaCl at an initial concentration of 16 to 18 mg/ml. Peptide 1 was less soluble than peptide 2. Insoluble material was removed by centrifugation, and both peptides were passed over a Superdex 75 gel filtration column. The main peak fractions were pooled and concentrated using YM-3 Microcon devices (Millipore), and the total protein concentration was determined by a standard bicinchoninic acid assay (Pierce). For dynamic light scattering experiments, samples were used at a final concentration of 6 mg/ml. Measurements were performed with a DynaPro machine (Viscotek Corp., Houston, Tex.) and analyzed by monomodal analysis, since both samples were found to be monodisperse. In calculations of their hydrodynamic radii, the elongated shapes of the peptides were accounted for by choosing the model "coils." For the molecular weight (MW) estimation, the volume shape hydration relationship model was used.

**Expression, purification, and refolding of an N-terminally tagged GP-2 ectodomain construct (GP-2ecto).** An *Escherichia coli* codon-optimized sequence coding for a N-terminal $His_6$ tag fused to amino acid (aa) 312 to aa 435 of LCMV-WE GP with a C316S point mutation was synthesized (Entelechon, Regensburg, Germany). The sequence was cloned into the pET-19b vector (Novagen, Madison, WI) and expressed in the cytoplasm of *E. coli* strain BL21(DE3) pLysS. The recombinant protein contained in inclusion bodies was separated from the cell lysate by centrifugation, resolved in 8 M urea, and purified by Ni-nitrilotriacetic acid affinity chromatography (Amersham Biosciences). Purified urea-denatured protein was refolded by a 1:100 drop-by-drop dilution in ice-cold refolding buffer while stirring. After 48 h of continuous stirring at 4°C, the refolded protein was concentrated using an Amicon stirred cell (Millipore Corporation, Billerica, MA). Precipitated protein was removed by centrifugation, and the supernatant was passed over a Superdex 75 gel filtration column, thereby exchanging the buffer to phosphate-buffered saline (PBS), pH 7.0. Purified complexes were glutaraldehyde cross-linked for 10 min at room temperature (RT) and analyzed by sodium dodecyl sulfate-polyacrylamide gel electrophoresis (SDS-PAGE).

**Circular dichroism measurements.** All samples were purified by gel filtration chromatography immediately before being subjected to circular dichroism measurements with a Jasco J-715 spectropolarimeter (Jasco Corporation, Tokyo, Japan). The concentrations in PBS were 0.05 mg/ml, 0.05 mg/ml, and 0.075 mg/ml for peptide 1, peptide 2, and GP-2ecto, respectively. Spectra represent the averages of four individual scans and were recorded at 4°C with a step size of 10 nm.

**Generation of the GP fibritin fusion construct.** The GP fibritin fusion sequence was generated by a fusion PCR. The phage T4-derived fibritin sequence GYIPEAPRDGQAYVRKDGEWVLLSTFL (39) was amplified from a synthetic gene (Entelechon GmbH, Regensburg, Germany) by use of overhanging primers. The obtained 115-nucleotide-long PCR product was purified and used together with a primer annealing to the 3′ end of the GP sequence in a second fusion PCR to amplify the complete GP ectodomain sequence. The GP template plasmid contained a full-length human codon-optimized GP sequence and was a gift from Dorothee von Laer. The GP sequence used corresponded to the LCMV-WE amino acid sequence published by Beyer et al. (2). Prior to the GP amplification, the SKI-1/S1P cleavage site had been removed by a point mutation (R262A) (3). The product obtained by the fusion PCR was ligated into pGEMT (Promega) and sequenced. Finally, the sequenced PCR product was excised by BamHI sites, which had been introduced by the primers, and was cloned into the plasmid pHCMV-GP (WE) (AJ318513), replacing the original LCMV-WE GP sequence (2). The expression vector pHCMV contains the human cytomegalovirus immediate early promoter, the rabbit beta globin intron B, and the rabbit beta globin polyadenylation sequence as well as an ampicillin resistance gene.

**Generation of stable cell lines.** Human embryonic kidney (HEK) T293 cells were calcium phosphate transfected with the GP fibritin expression plasmid and the coplasmid pHygEGFP (where EGFP is enhanced green fluorescent protein) (DB Biosciences Clontech), carrying the hygromycin resistance gene for selection. After transfection, cells were grown adherently for 3 days in nonselective Dulbecco's modified Eagle's medium (Invitrogen) containing 10% fetal calf serum (FCS) before 0.3 mg/ml hygromycin B (Roche) was added. After 1 week of selection, dead cells were removed and adherent cells were trypsinized and transferred to a new flask. After expansion of the cells for at least 2 weeks, cells were subcloned in 96-well plates and cell supernatants were screened for secreted GP fibritin fusion protein (GPfib) by enzyme-linked immunosorbent assay. In brief, 96-well plates were coated with the GP-1-specific antibody KL25 at 5 μg/ml overnight at 4°C and were blocked with 5% milk diluted in phosphate-buffered saline containing 0.05% Tween (PBS-T). A portion (100 μl) of the cell supernatant was transferred to the coated plate and incubated for 1 h at RT. Bound GPfib was detected with 10 μg/ml biotinylated KL25 for 1 h at RT, followed by streptavidin-coupled HRP for 45 min at RT. Between each step, the

plates were washed with PBS-T. High producers were subjected to a second round of subcloning. Large-scale production was carried out in triple-layer tissue culture flasks with adherent cells. Cells were expanded in Dulbecco's modified Eagle's medium (Invitrogen) with 10% FCS until the cell monolayer was nearly confluent. For production, cells were washed once with PBS and kept in FCS-free InVitrus medium (Cell Culture Technologies GmbH, Gravesano, Switzerland), supplemented with 0.5 mM sodium butyrate (Fluka). GPfib-containing cell supernatant was collected twice, after 2 and 4 weeks.

**Purification of GPfib.** Concentrated serum-free cell supernatant was filtered through a 0.2-μm filter (Millipore) before being passed over a KL25 affinity column. Bound GPfib was eluted with 0.1 M glycine buffer, pH 2.7, and immediately neutralized with 1 M Tris-HCl, pH 7.0. To prepare the antibody affinity column, the carbohydrate side chains of the antibody were oxidized with 10 mM sodium metaperiodate (Sigma) in 0.1 M sodium phosphate buffer, pH 5.5, for 45 min at 4°C in the dark. The reaction was stopped by the addition of 15 mM glycerol, and the oxidized carbohydrates were reacted with 50 mM biotin-LC-hydrazide (Pierce) for 3 h at RT on an end-over-end rotor. Unreacted biotin-hydrazide was removed using a 5-ml HiTrap desalting column (Amersham Biosciences), and the biotinylated antibody was bound to a 5-ml HiTrap streptavidin HP column (Amersham Biosciences). After KL25 affinity chromatography, purified GPfib was concentrated to a final volume of 0.2 ml by use of YM-50 Microcon filter devices (Millipore) before being passed over a Superdex 200 HR10/30 gel filtration column (Amersham Biosciences). The flow rate was 0.5 ml/min, and the running buffer was either 20 mM HEPES, pH 7.0, or PBS. For calibration of the Superdex 200 HR10/30 column, a high-molecular-weight gel filtration calibration kit from Amersham Biosciences was used.

**SDS-PAGE and immunoblotting with the antibodies KL25, Wen3, Wen4, WE 18.8, and WE 83.4.** Samples were analyzed nondenatured, denatured, partially reduced, or completely reduced. Nondenatured-sample preparation included addition of SDS sample buffer without heating prior to loading. Denatured-sample preparation included heating (10 min at 95°C). Partially reduced-sample preparation included addition of 10 mM dithiothreitol (DTT) to the sample for 10 min at room temperature before addition of SDS sample buffer and loading. Completely reduced-sample preparation included addition of SDS sample buffer with 150 mM DTT and heating. All samples were separated by SDS-PAGE at room temperature, and proteins were transferred to nitrocellulose membranes by wet blotting overnight at 4°C. Blots were blocked with 5% milk in PBS-T for at least 3 h before being incubated either with KL25, Wen3, or Wen4 (all at 10 μg/ml) or with WE 18.8 and WE 83.4 ascites fluids (diluted 1:1,000) for 2 h. Detection was carried out with HRP-coupled isotype-specific antibodies, diluted 1:1,000 in PBS-T. All steps were carried out at 4°C, and the blots were washed six times for 5 min with PBS-T between each step. HRP was detected using an enhanced chemiluminescent substrate (Pierce).

**Glutaraldehyde cross-linking.** KL25 affinity-purified and Superdex 200 gel filtration-purified GPfib in 20 mM HEPES, pH 7.0, was concentrated with YM-50 Microcon devices (Millipore) to a final concentration of around 1 mg/ml. Five-microliter drops were distributed into Eppendorf tubes, and 0.5-μl drops of 10× glutaraldehyde stock solutions were added. The final glutaraldehyde concentrations ranged from 0.015% to 2%. After incubation for 15 min at RT, the reaction was stopped by addition of 10 μl 0.5 M Tris-HCl, pH 7.0. Finally, 5 μl reducing SDS sample buffer was added and the samples were immediately boiled for 5 min at 99°C before being separated by SDS-PAGE.

**Electron microscopy.** GPfib was affinity purified and passed over a Superdex 200 gel filtration column, thereby exchanging the buffer to 20 mM HEPES, pH 7.0. Fractions containing peak A were pooled and concentrated with YM-50 Microcon devices (Millipore). Five-microliter drops were applied to carbon-coated gold grids, which had been glow discharged before. The absorbed protein was stained with 2% phosphor-wolfram acid, pH 7.2. Micrographs were recorded with a Philips model CM12 electron microscope.

## RESULTS

**Sequence analysis of the GP-2 subunit reveals a trimeric heptad repeat pattern.** Secondary structure prediction (34) for the LCMV-WE GP-2 sequence identified two extended α-helical regions (Fig. 1A). One region ranged from aa 313 to aa 365 (helix 1), and the other ranged from aa 402 to aa 429 (helix 2). Both predicted α-helices are thought to be connected by a disulfide-bonded loop between cysteines 370 and 391 (27). The program LearnCoil-VMF, which was especially trained to identify heptad repeat patterns in trimeric viral glycoproteins (48), revealed a heptad repeat pattern within helix 1, ranging from aa 334 to aa 365 (Fig. 1B). To validate our findings on the LCMV GP-2 sequence, we extended the examination to other Old and New World arenavirus family members. Aligned sequence analysis showed that both the positions of helices 1 and 2 and the heptad repeat pattern within helix 1 were highly conserved. Furthermore, it allowed us to define the boundaries of the heptad repeat pattern more precisely and established a longer sequence, ranging from aa 327 to aa 365. Taken together, the findings predicted that the N-terminal helix 1 within the arenavirus GP-2 subunit would form a trimeric coiled-coil core. This feature is a hallmark of viral class I fusion proteins.

**A peptide corresponding to the N-terminal helix 1 of GP-2 forms a stable oligomer.** To assess the secondary structure and oligomerization potential of the postulated helices 1 and 2 experimentally, we generated synthetic peptides corresponding to each region. Peptide 2 comprised aa 404 to aa 428 of helix 2 and had a molecular mass of 3.3 kDa (Fig. 2C). Peptide 1 comprised aa 325 to aa 354 of the heptad repeat pattern containing helix 1 and had a molecular mass of 3.1 kDa (Fig. 2B). Circular dichroism measurements indicated that both peptides adopted α-helical structures when dissolved in PBS at pH 7.0 (Fig. 2E and F). While the spectrum of peptide 2 revealed predominantly α-helical elements, peptide 1 was found to be entirely α-helical. The findings for peptide 1 are in agreement with a previous study of a similar, LCMV-Armstrong-4-derived peptide (27). Because of their similar MWs and secondary structures, peptide 1 and peptide 2 were expected to be similar in shape. However, they displayed distinct elution profiles by gel filtration chromatography (Fig. 2G). Peptide 2 eluted as one sharp peak, while peptide 1 displayed only a minor peak at the same position. The major peak of peptide 1, accounting for about 90% of the total material, was shifted to a higher-molecular-weight fraction. This observation indicated that peptide 1, in contrast to peptide 2, was able to form an oligomer stable enough to endure gel filtration. In order to determine the hydrodynamic radii of both peptides in solution, fractions corresponding to the main peaks of both peptides were subjected to dynamic light scattering experiments. Both peptide solutions were found to be monodisperse, and the average particle radius was determined by monomodal analysis to be 2.05 nm for peptide 1 and 1.47 nm for peptide 2 (Table 1). For molecular mass calculation of the particles, the volume shape hydration relationship model was applied, and it yielded a hypothetical molecular mass of 18.7 kDa for peptide 1 particles and of 6.8 kDa for peptide 2 particles. Since the molecular mass calculation model used was based on globular particles, the absolute molecular mass values obtained for the ellipsoid peptide particles were not accurate. However, since both peptides formed helices in solution and were thus expected to be similar in shape, the MW ratio (peptide 1 particles/peptide 2 particles = 2.8) suggested the possibility that peptide 1 might form trimers. In summary, the observed behavior of peptide 1 and peptide 2 was consistent with our in silico predictions.

**A GP-2 ectodomain fragment corresponding to aa 313 to aa 435 forms stable trimers and adopts an entirely α-helical structure.** To further assess whether the GP-2 domain behaved in a manner similar to that of the transmembrane subunits of class I viral fusion proteins, we extended our study from iso-

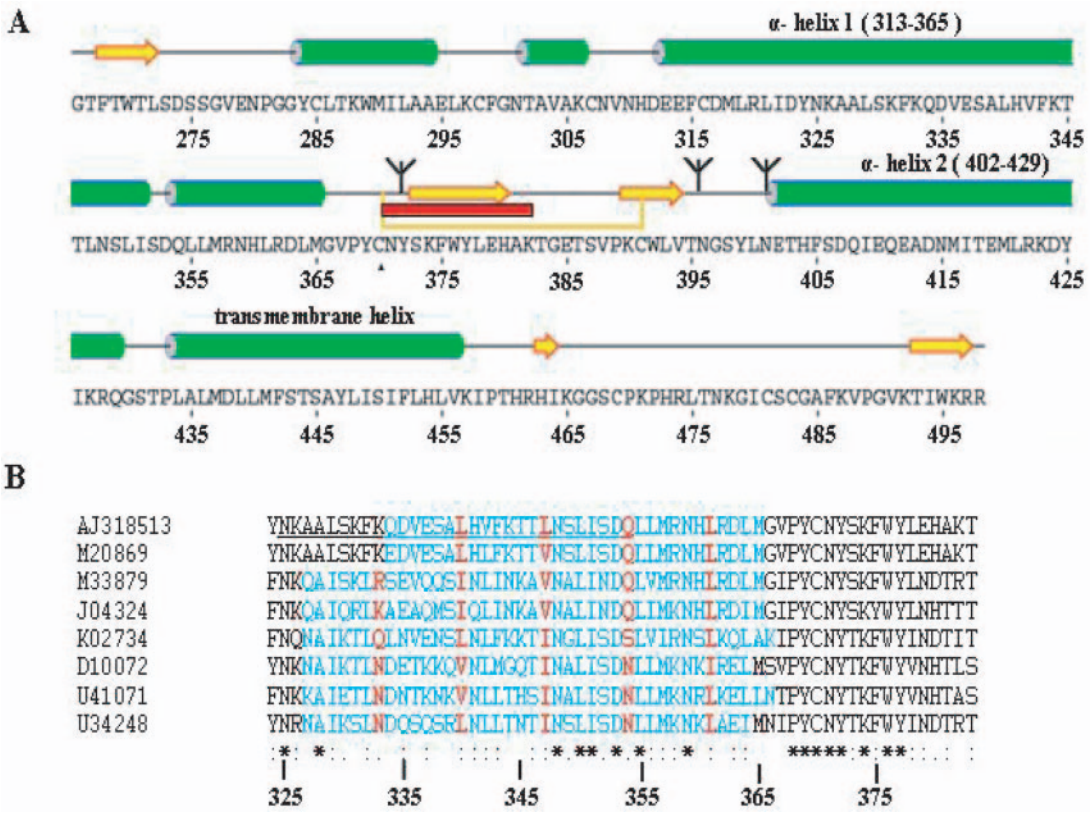


FIG. 1. Secondary structure prediction of the GP-2 subunit and identification of a trimeric heptad repeat pattern. (A) Secondary structure prediction for the LCMV-WE GP-2 sequence (AJ318513) used in this study (34). Green cylinders represent predicted α-helices, and yellow arrows represent β-sheets. Three prominent α-helices were identified: α-helix 1 ranged from aa 313 to aa 365, and α-helix 2 ranged from aa 402 to aa 429, located just prior to the transmembrane helix (10). A predicted disulfide-bonded loop is indicated by a yellow line connecting cysteines 370 and 391. N-linked glycosylation sites are indicated by trees. The major antigenic site on GP-2 (aa 371 to aa 382), which is recognized by the antibody WE 83.4, is highlighted in red (54). (B) Results of the LearnCoil-VMF analysis for aligned sequences of LCMV-WE (AJ318513), LCMV-Armstrong (M20869), Mopeia (M33879), Lassa (J04324), Pichinde (K02734), Junín (D10072), Sabia (U41071), and Oliveros (U34248) viruses (48). Sequences containing a potential trimeric heptad repeat pattern are highlighted in blue. Amino acids in the α-position within the heptad repeat pattern are colored in red. The underlined stretch within the LCMV-WE sequence (AJ318513) matches the sequence of peptide 1, which was tested for its oligomerization potential. The degree of conservation among the aligned sequences is indicated at the bottom: an asterisk indicates complete conservation, and two dots and one dot indicate more-conservative mutations with respect to charge and size.

lated peptides to the complete GP-2 ectodomain. A GP-2 sequence comprising the whole heptad repeat pattern containing helix 1, the disulfide-bonded loop region, and helix 2 was expressed in *E. coli* (Fig. 2D). To avoid aggregation, the hydrophobic N-terminal fusion peptide was omitted from the construct, and cysteine 316 was replaced by serine to prevent artificial interchain disulfide bond formation in the absence of cysteines 285, 298, and 307. The construct, designated GP-2ecto, was purified from inclusion bodies in a urea-denatured state by affinity chromatography and refolded by rapid dilution. Gel filtration analysis revealed a single peak at a volume identical to that of ovalbumin (43 kDa), markedly differing from the molecular mass of monomeric GP-2ecto (15 kDa) (data not shown). To determine the precise oligomerization state of GP-2ecto, a glutaraldehyde cross-linking experiment was performed (Fig. 3A). Three bands migrating at the expected sizes of monomers (15 kDa), dimers (30 kDa), and trimers (45 kDa) were identified. The maximal band intensity shifted from the monomer band to the trimer band with increasing glutaraldehyde concentrations. No band corresponding to a tetramer was observed. Circular dichroism spectroscopy confirmed an all-alpha protein structure (Fig. 3B). In summary, we found the GP-2ecto construct to behave remarkably similarly to the transmembrane subunits of class I viral fusion proteins. When expressed without their receptor binding subunits, these proteins are known to spontaneously adopt an all-alpha trimeric six-helix bundle conformation.

**The uncleavable LCMV GP ectodomain can be expressed as fibritin fusion protein.** Based on the observed trimeric nature of the GP-2 fragment, we chose an expression strategy for the complete LCMV GP ectodomain that had previously proven successful for similarly organized trimeric viral glycoproteins (49, 52, 56). The whole LCMV-WE GP ectodomain (aa 1 to aa 430) was fused at its C terminus to a fibritin-derived trimerization motif replacing the transmembrane helix and cytoplasmic tail (Fig. 4A). The 27-aa-long fibritin sequence employed is known to form a hairpin-like structure and has the potential to stabilize trimeric complexes (39). To inhibit proteolytic processing of GPfib, we introduced a point mutation (R262A) at the subtilase SKI-1/S1P consensus site (3). T293 cells were

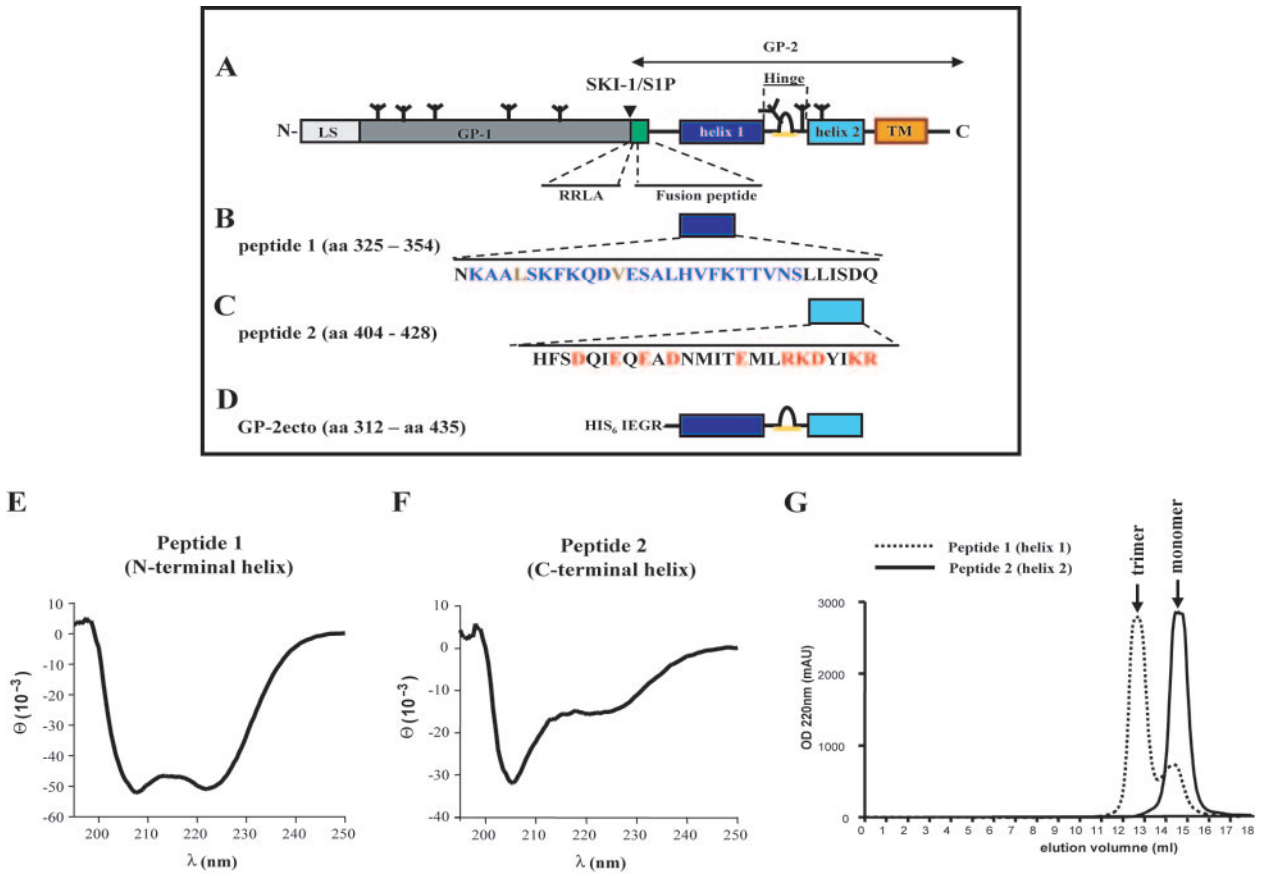


FIG. 2. An α-helical peptide corresponding to the heptad repeat pattern containing helix 1 forms stable oligomers at pH 7.35, whereas an α-helical peptide corresponding to helix 2 has no potential to oligomerize. (A) Wild-type LCMV-WE GP sequence. At the N terminus, the leader sequence (LS) is indicated, followed by the receptor binding subunit GP-1 and the transmembrane subunit GP-2. N-linked carbohydrates are indicated by trees. The subtilase SKI-1/S1P cleavage site and the corresponding consensus sequence (RRLA) are marked by an arrowhead. Structural features within the GP-2 subunit are highlighted: the predicted N-terminal hydrophobic fusion peptide is colored in green (29, 30), the identified heptad repeat pattern containing α-helix 1 in dark blue, and α-helix 2 in light blue. Helices 1 and 2 are connected by a hypothetical disulfide-bonded loop (27). At the very C terminus, the transmembrane helix (TM) and the cytoplasmic tail are shown. (B and C) Full-length sequences of peptides used in this study. Amino acids in the peptide 1 sequence, which have been identified by the LearnCoil-VMF program, are colored in blue. Charged amino acids in the peptide 2 sequence are colored in red, thus emphasizing the strong amphipathic character of this helical region. (D) N-terminally tagged GP-2 ectodomain construct (GP-2ecto) expressed in *E. coli*. The construct contained a C316S point mutation to avoid artificial interchain disulfide bridges. (E and F) Circular dichroism spectra for peptide 1 and peptide 2, respectively. (G) Superdex 75 gel filtration chromatograms for peptide 1 (3.1 kDa) and peptide 2 (3.3 kDa) at pH 7.35. Peptide 1 shows a main peak at an elution volume of 13 ml and a minor shoulder peak at 15 ml, whereas peptide 2 shows a single peak at 15 ml. The main peak fractions of each peptide were concentrated and analyzed by dynamic light scattering. OD 220nm, optical density at 220 nm; mAU, milli-adsorption units.

TABLE 1. Measurements of peptide 1 and peptide 2 particles

| Parameter | Value for[a]: | |
|---|---|---|
| | Peptide 1 particles | Peptide 2 particles |
| Hydrodynamic radius (nm) | 2.05 | 1.47 |
| Polydispersity (nm)[b] | 0.3 | 0.3 |
| Molecular mass (kDa)[c] | 18.7 | 6.8 |

[a] Peptide 1 particles form stable trimers at pH 7.35, as revealed by dynamic light scattering. For peptide 1 particles, the mean scattering amplitude of the measurement was 0.798, and the diffusion coefficient was 1,025 $cm^2/s$. For peptide 2 particles, the mean scattering amplitude of the measurement was 0.670, and the diffusion coefficient was 1,434 $cm^2/s$.

[b] The peptide 1 sample is primarily monodisperse, since the polydispersity is 14.0% of the mean hydrodynamic radius. Monomodal analysis yields a baseline of 1.000 and a sum-of-squares value of 0.387. The peptide 2 sample is primarily monodisperse, since the polydispersity is 20.0% of the mean hydrodynamic radius. Monomodal analysis yields a baseline of 1.000 and a sum-of-squares value of 2.726.

[c] The molecular masses of the particles were calculated by applying the volume shape hydration relationship model using a standard curve of globular proteins.

stably transfected with the fusion construct and screened for highly producing subclones by enzyme-linked immunosorbent assay using the monoclonal antibody KL25. GPfib-containing cell supernatant was initially characterized by Western blot analysis with a panel of monoclonal antibodies directed against various GP-1 and GP-2 epitopes. KL25, Wen3, and Wen4 are neutralizing antibodies binding to the conformational GP-1A epitope, whereas the antibodies WE 18.8 and WE 83.4 are directed against the linear epitopes GP-1C and GP-2A (42). All antibodies recognized two distinct bands if the samples had been resolved by SDS-PAGE under mild conditions (Fig. 4B). The position of the lower band, migrating between 150 and 250 kDa, corresponded well to the theoretical molecular mass of a trimeric GPfib complex including carbohydrates (210 kDa). Since the upper band above 250 kDa had barely entered the separating gel, a more precise molecular mass determination

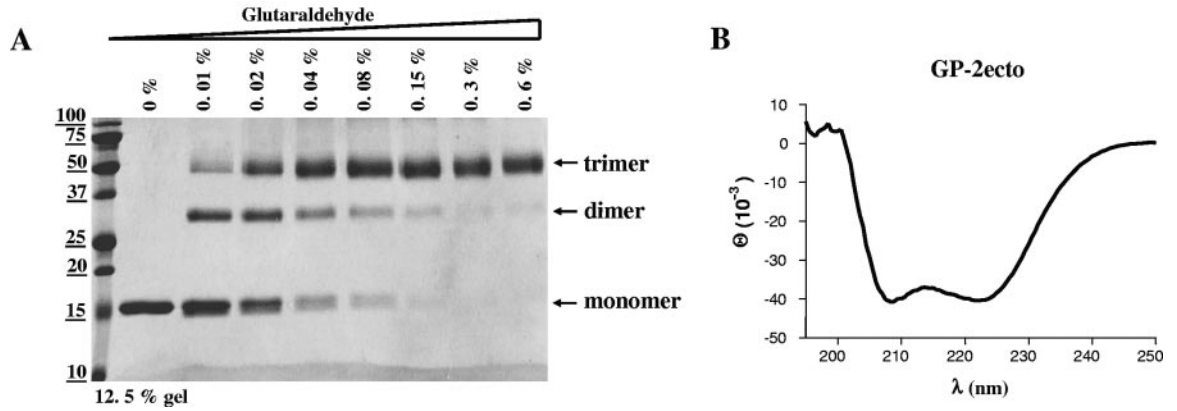


FIG. 3. GP-2ecto forms stable trimers and adopts an entirely α-helical structure. GP-2ecto was expressed in *E. coli* and purified from inclusion bodies by Ni-nitrilotriacetic acid affinity chromatography. The urea-denatured protein was refolded by rapid dilution, and reconstituted GP-2ecto complexes were separated by Superdex 75 gel filtration chromatography. (A) Glutaraldehyde cross-linking analysis of the gel filtration-purified GP-2ecto complexes. Cross-linking was carried out for 10 min at room temperature. Monomeric GP-2ecto has a theoretical molecular mass of 15 kDa. Molecular mass markers (in kDa) are noted at the left of blots. (B) Circular dichroism spectrum for the GP-2ecto complexes, which was recorded in PBS, pH 7.0, at 4°C immediately after gel filtration purification.

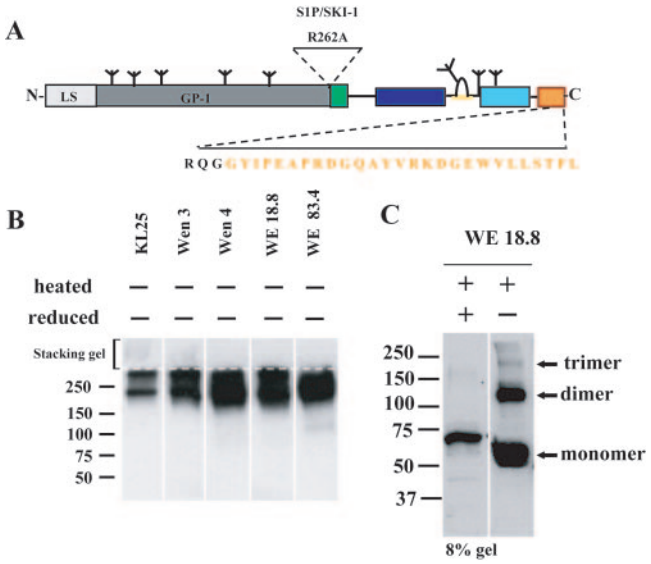


FIG. 4. T293 cells secrete two distinct GPfib complexes, which contain interchain disulfide bridges. (A) Uncleavable GP fibritin fusion construct. The transmembrane helix and the cytoplasmic tail were replaced by the 27-aa-long trimeric motif of bacteriophage T4-derived fibritin. At the fusion site, two additional glycine residues were introduced to increase the overall flexibility in the linker region. To avoid proteolytic processing, the subtilase SKI-1/S1P consensus sequence was mutated (R262A). HEK T293 cells were stably transfected and subcloned. (B) Nondenaturing Western blot analysis of serum-free cell supernatant. Detection was carried out with the monoclonal antibodies KL25, Wen3, Wen4, WE 18.8, and WE 83.4. KL25, Wen3, and Wen4 bind to the conformational and reduction sensitive epitope GP-1A on GP-1. The antibodies WE 18.8 and WE 83.4 bind to the linear epitopes GP-1C on GP-1 and GP-2A on GP-2, respectively (42). The border of the stacking gel is indicated by a dotted line. Minuses above the blots indicate absence of heat and reduction. (C) Western blot analysis of serum-free cell supernatant with the antibody WE 18.8, when the sample was either completely reduced (lane 1) or heat denatured without reduction (lane 2). Molecular mass markers (in kDa) are noted at the left of blots.

was impossible. No other bands were detected with any of the antibodies, demonstrating that exclusively GPfib complexes were secreted. If the samples were reduced and boiled in SDS, the antibody WE 18.8 detected a single band of the expected size of monomeric GPfib (70 kDa) (Fig. 4C, lane 1). However, if the sample was boiled in SDS without reduction, an additional prominent band of ~140 kDa and two very weak bands, above 150 kDa and 250 kDa, became apparent (Fig. 4C, lane 2). These bands are likely to represent disulfide-linked dimers, trimers, and tetramers of GPfib and led to the conclusion that interchain disulfide bonds exist within the secreted complexes. Furthermore, an upward shift of the GPfib monomer band upon complete reduction was observed. A similar shift had been reported before, when the GP-1 subunit from purified virus had been analyzed (6, 12).

**GPfib forms two distinct complexes of ~230 kDa and ~440 kDa which can be converted to a single ~250-kDa species by partial reduction.** GPfib was purified from the cell supernatant by affinity chromatography and analyzed by SDS-PAGE and Coomassie staining. As observed before by Western blotting (Fig. 4B), samples exposed to mild conditions contained no bands corresponding to monomers or dimers but several bands migrating around 250 kDa (Fig. 5A). It is interesting to note that when the sample was partially reduced by 10 mM DTT for 10 min at room temperature, all bands observed before were converted to a single band of exactly 250 kDa [Fig. 5B, band A (red)]. This demonstrated that the migration behavior of the different complex species was due to surface-exposed disulfide bonds. To further investigate the molecular masses of the different complex species, purified GPfib was subjected to gel filtration chromatography (Fig. 5C). As expected, two peaks could be resolved. The elution volume of the major peak, peak A, was close to that of catalase (232 kDa), while the elution volume of the minor peak, peak B, was comparable to that of ferritin (440 kDa). The eluted fractions were split in half and either partially reduced or not before being analyzed by 5% SDS-PAGE and Western blotting. The nonreduced samples allowed us to assign the ~440-kDa complex (Fig. 5C, peak B)

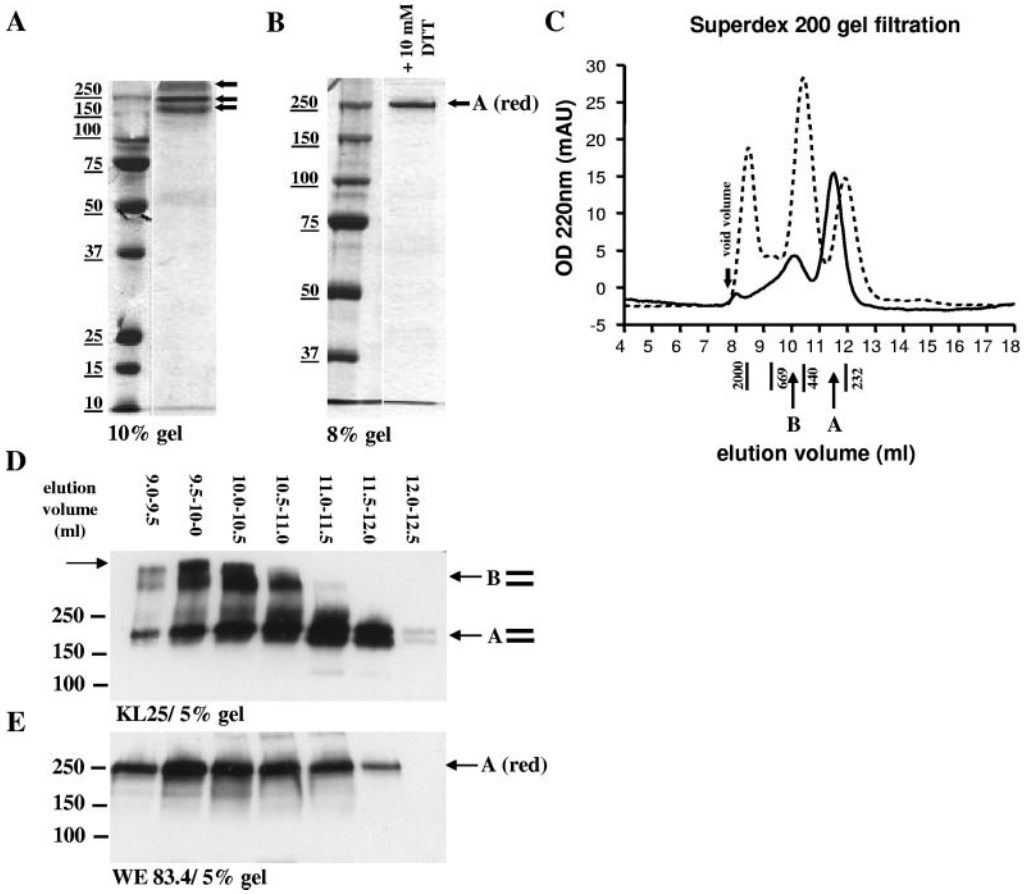


FIG. 5. GPfib forms two complexes of ~230 and ~440 kDa, which upon partial reduction are converted to a single complex species migrating at exactly 250 kDa. GPfib complexes were purified from the cell supernatant by affinity chromatography and analyzed by SDS-PAGE and Coomassie staining. (A) Native nondenatured complexes, when the sample was neither reduced nor heated. (B) Same sample as that shown in panel A, but partially reduced with 10 mM DTT for 10 min at room temperature. (C) Superdex 200 gel filtration chromatogram for 50 μg of affinity-purified GPfib complexes (solid line). Furthermore, a column calibration with catalase (232 kDa), ferritin (440 kDa), thyroglobulin (669 kDa), and dextran blue (2,000 kDa) is shown (dotted line). OD 220nm, optical density at 220 nm; mAU, milli-adsorption units. (D and E) Fractions 11 to 17 of the gel filtration separation were resolved by 5% SDS-PAGE and analyzed by Western blotting. Samples were loaded either nondenatured (D) or partially reduced (E), and detection was carried out with KL25 (D) or WE 83.4 (E), respectively. Molecular mass markers (in kDa) are noted at the left of blots.

to the upper band (Fig. 5D, band B), migrating above 250 kDa. The ~230-kDa complex (Fig. 5C, peak A) was assigned to the lower band (Fig. 5D, band A), migrating between 150 and 250 kDa. Both complex species (Fig. 5C, peaks A and B) were migrating as double bands for an unknown reason (Fig. 5D). Upon partial reduction, all four bands merged again into one band migrating at exactly 250 kDa [Fig. 5E, band A (red)]. This band was still recognized by the antibody WE 83.4, but it had lost the GP-1A epitope, since it was no longer detectable with the antibody KL25 (data not shown). We concluded that the 440-kDa complex (Fig. 5C, peak B, and D, band B) was most likely a disulfide-bonded dimer of the 230-kDa complex (Fig. 5C, peak A, and D, band A). Furthermore, partial reduction seems to open a surface-exposed intrachain disulfide bond within the GP-1 subunit. This would account for the loss of the neutralizing GP-1A epitope (55) and can explain the observed upward shift of the 230-kDa complex to 250 kDa upon partial reduction [compare Fig. 5D, band A, and E, band A (red)].

**Glutaraldehyde cross-linking demonstrates the trimeric state of the 230-kDa complex.** The apparent molecular mass of the 230-kDa complex strongly suggested that it represented GPfib trimers. To assess the oligomeric state of the 230-kDa complex experimentally, we performed a cross-linking experiment (Fig. 6). Aliquots of the gel filtration-purified 230-kDa complex (Fig. 5C, peak A) were incubated with increasing concentrations of glutaraldehyde for 15 min at room temperature and were subsequently analyzed by reducing SDS-PAGE. In addition to the monomer band that was observed exclusively in the absence of glutaraldehyde, two more bands, of ~140 kDa and ~210 kDa, emerged upon cross-linking. Judged by their molecular masses, these bands represented dimers and trimers of GPfib. The relative intensities of the three bands changed with increasing glutaraldehyde concentration. At 0.01% the dimer band was most intense, while the trimer band became dominant at 0.03%. Above this concentration, the cross-linking was complete since only trimers could

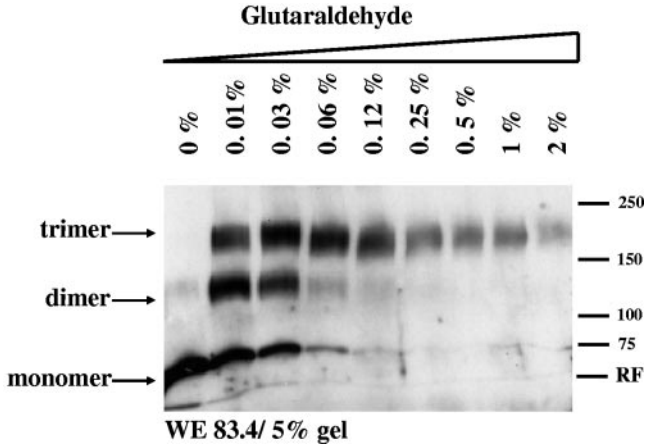


FIG. 6. Glutaraldehyde cross-linking demonstrates the solely trimeric state of the 230-kDa complexes. Affinity-purified and gel filtration-separated 230-kDa complexes were glutaraldehyde cross-linked for 15 min at room temperature before the reaction was stopped. Samples were completely reduced, separated by 5% SDS-PAGE, and analyzed by Western blotting with the antibody WE 83.4. If the glutaraldehyde concentration was raised above 0.06%, the trimer band slowly faded away, since the WE 83.4 epitope is known to contain a lysine residue (54). Molecular mass markers (in kDa) are noted at the right of blots. RF indicates the running front of the gel.

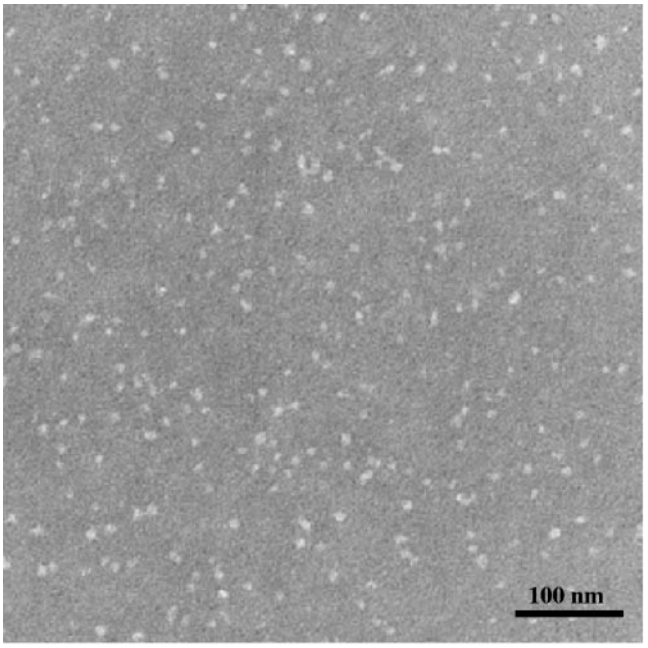


FIG. 7. Purified 230-kDa trimers appear as spherical particles of 10 nm in length and 7 nm in width. Affinity- and gel filtration-purified 230-kDa complexes were analyzed by negative-contrast electron microscopy. Purified complexes in 20 mM HEPES buffer, pH 7.0, were adsorbed to carbon-coated gold grids and stained with 2% phosphorwolfram acid. Micrographs were recorded with a Philips model CM12 electron microscope. Neither aggregates nor rosette formations of the complexes were observed.

be observed. No bands corresponding to higher oligomers, such as tetramers, were detected. This finding clearly demonstrated the trimeric nature of the 230-kDa complex. Consequently, the 440-kDa complex, which was converted to a 250-kDa species upon partial reduction, represented a disulfide-linked pair of trimers.

**GPfib forms single spherical particles.** Gel filtration-purified GPfib trimers were imaged by negative-stain electron microscopy (Fig. 7). The particles exhibited a spherical shape, were equally distributed, and showed no signs of rosette formation. The dimensions of the GPfib particles were ~10 nm in length and ~7 nm in width. Micelle or rosette formation has been described for many other purified viral glycoprotein spikes and is thought to occur if the N-terminal hydrophobic fusion peptide of the transmembrane subunit becomes exposed to the solvent (13, 15, 43). The absence of rosettes thus implies that the GPfib trimer resembles the GP spike in its preactivated prefusion state. This was expected since the GPfib trimer was stabilized both by the mutation of the cleavage site and by the addition of the fibritin domain.

## DISCUSSION

In this study, we have analyzed the oligomeric state of the LCMV GP. Sequence analysis of the transmembrane subunit GP-2 identified two prominent α-helices and revealed a trimeric heptad repeat pattern within the N-terminal helix. Peptides matching the identified helices were found to be α-helical in solution. The peptide corresponding to the N-terminal helix spontaneously oligomerized in solution, whereas the peptide corresponding to the C-terminal helix failed to oligomerize. When applying a refolding protocol to the complete GP-2 ectodomain (aa 324 to aa 435), we obtained stable trimeric complexes. The reconstituted trimers were all-alpha structures, thus resembling six-helix bundles of other viral class I glycoproteins. Therefore, we fused the uncleavable LCMV GP ectodomain to fibritin and expressed it in T293 cells. We demonstrated that the fusion protein was secreted from the cells exclusively as a trimer and that it was recognized by various antibodies binding to conformational and sequential epitopes within the GP-1 and GP-2 subunits. The recombinant trimers resembled the previously described spikes of LCMV virions with respect to their dimensions and shape (41).

These findings allow us to revisit the classification of the LCMV GP. Until now, its assignment to class I viral membrane fusion proteins was problematic, since it did not satisfy all characteristics of this class (23, 35). In line with the class I criteria, the LCMV GP consists of a receptor binding subunit noncovalently attached to the transmembrane subunit (4, 10). Both are generated from a common precursor protein through cleavage by a cellular protease (3, 11, 38). The mature LCMV spike is in a metastable state, which can undergo an acid-triggered conformational change (18, 19). In electron microscopy, the spikes appear as relatively long projections perpendicular to the viral membrane (41). However, in striking contrast with the class I architecture, cross-linking experiments with whole virions indicated that the LCMV GP formed tetrameric spikes (12). The present study allows us to overcome this dilemma by presenting strong experimental evidence for the trimeric state of the LCMV GP. We therefore propose a model of the LCMV GP which is based on the general class I architecture (17, 20, 21, 24, 31, 33, 46, 50) and integrates

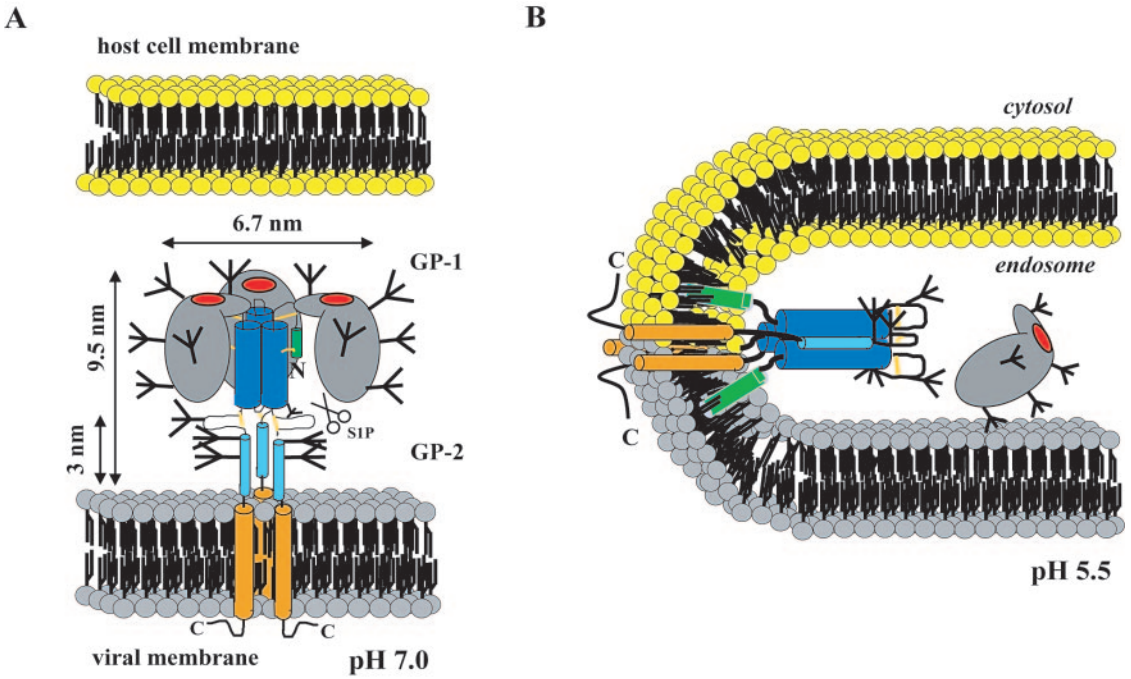


FIG. 8. Proposed class I model of the arenavirus GP. (The color coding is identical to that used in Fig. 2A; the indicated dimensions have been adopted from a recent electron cryomicroscopy study [41].) (A) Arenavirus GP spike in its hypothetical prefusion state. The model is based on published data on the LCMV-WE GP and on data obtained in this study as well as on the general model of class I viral fusion proteins. The pH-sensitive GP spike is shown as a trimer of GP-1/GP-2 heterodimers, which has been activated upon proteolytic processing by the subtilase SKI-1/S1P (3, 11, 38). GP-1 forms the globular head subunit, whereas GP-2 forms the membrane fusion-mediating subunit. GP-1 is covered by a dense carbohydrate shield, with the exception of the receptor binding site, depicted in red (4, 55). Neutralizing antibodies bind exclusively to this surface area, thus blocking receptor binding (4, 16, 42). The receptor for the arenaviruses is α-dystroglycan (4, 14, 51). GP-1 acts as a novel lectin, binding to yet-unidentified sugar moieties on *O*-mannosyl-linked carbohydrates (32, 36). The 3-nm-long stalk region of the spike is made up of the highly charged α-helix 2 region and a hypothetical disulfide-bonded loop (27). Three N-linked carbohydrates within this region (depicted as trees) (55) and the finding that the disulfide-bonded loop is surface exposed on infectious virions (42) support the suggested topology. The N-terminal half of the GP-2 ectodomain, including the coiled-coil core and the N-terminal hydrophobic fusion peptide (29, 30), is buried in the interior of the complex to keep the spike in its fusion-competent state. (B) GP spike in its hypothetical low-energy postfusion state, after formation of the viral fusion pore. The membrane of the infected host cell is colored in yellow and the viral membrane in light gray. The GP-2 subunit is shown in its predicted six-helix bundle conformation; thus, the α-helix 2 packs in an antiparallel fashion into the grooves of the N-terminal coiled-coil core. This step is thought to occur in early endosomes at pH 5.5, since a low pH is needed for destabilizing the trimer by release of the GP-1 subunit (18, 19, 41).

previous data on the LCMV GP, as well as the findings presented in this study.

Figure 8A depicts a model of the LCMV GP spike in its metastable prefusion state as it is thought to exist on infectious virions. Each spike is built of three GP-1/GP-2 heterodimers, where GP-1 forms the globular head of the GP spike (41). Most likely, GP-1 makes up the major part of the spike's surface because this subunit is highly glycosylated, with evenly distributed glycans accounting for about 35% of its total mass (55). Furthermore, GP-1 accommodates the receptor binding site, which needs to be accessible on the virus surface (4). This site is known to be the only target site for virus-neutralizing antibodies, which are thought to inhibit receptor binding (4, 42). Four highly variable surface-exposed regions in the GP-1 sequence, most likely in close proximity to the receptor binding site, have been characterized. These regions were identified by sequencing of LCMV escape mutants evading a strong and focused neutralizing humoral immune response in mice (16).

There is evidence for the presence of disulfide-linked GP-1 subunits on purified infectious LCMV virions (12). It is interesting to note that interchain disulfide bonds between neighboring GPfib trimers and eventually within GPfib trimers were also identified in this study. Although further thorough analysis of these interchain disulfide bonds is needed, it is tempting to speculate that they could play a role during viral entry. Recent findings with other class I fusion proteins suggest that disulfide bond isomerizations are critically involved in the onset of membrane fusion. Inhibitors of protein disulfide isomerase were found to block human immunodeficiency virus type 1 entry (1, 28, 44). For Moloney murine leukemia virus, it was shown that isomerization of interchain disulfide bonds critically controls the fusion activity of the spike (53).

Figure 8A depicts the transmembrane subunit GP-2 as the stem of the GP spike, with its essential features highlighted. Whereas the N-terminal half of the GP-2 ectodomain is believed to be buried in the interior of the complex, the C-terminal half builds the 3-nm-long stalk region observed by electron cryomicroscopy (41). The stalk is surface exposed and comprises the hypothetical disulfide-bonded loop as well as the helix 2 region, which is located just prior to the transmembrane helix. The suggested topology is supported by the presence of three N-linked glycans within the C-terminal half of GP-2 (55)

and by an extensive epitope-mapping study, revealing a single antigenic site on GP-2, located within the disulfide-bonded loop (42, 54). The helix 2 region is imaged to adopt an overwhelmingly α-helical structure at pH 7.0, as demonstrated in this study. Furthermore, the helix 2 region is highly charged and amphipathic in character. This was also reflected by the high solubility of peptide 2 compared to the strongly hydrophobic peptide 1 (data not shown). The N-terminal half of the GP-2 ectodomain comprises the hydrophobic fusion peptide situated at the very N terminus (29, 30) as well as the trimeric coiled-coil core formed by helix 1. Both need to be buried within the GP-1/GP-2 complex to preserve the metastable prefusion state. Upon exposure to low pH, the high-energy prefusion state is destabilized, leading to the release of the GP-1 subunit from the GP spike (18, 19). As a consequence, the hydrophobic fusion peptide becomes exposed and inserts into the target membrane. Furthermore, the GP-2 subunit undergoes a series of conformational rearrangements leading to the postfusion six-helix bundle conformation (Fig. 8B). This low-energy state is formed by the C-terminal helices packing in an antiparallel manner into the hydrophobic grooves of the coiled-coil core. Thus, the N terminus and the C terminus of GP-2 are drawn together and give rise to the fusion pore.

The model we propose for LCMV can be extended to the other arenavirus family members based on their sequence similarity. Thus, the group of class I viral membrane fusion proteins comprises to date the arenavirus, the retrovirus, the filovirus, the coronavirus, the paramyxovirus, and the orthomyxovirus families (23, 35). Obviously, further structural work with the arenavirus GP is needed to understand the fusion process in detail. The GP-2ecto and the GPfib constructs presented in this study will be used in crystallization trials. A structure of the postulated six-helix bundle will be of especially great interest since it may stimulate the development of peptide-based or small-compound fusion inhibitors. Taken together, these studies will pave the way for antiviral strategies against a group of emerging human pathogens.

## ACKNOWLEDGMENTS

We thank Thomas Bächi (Elektronenmikroskopisches Zentrallabor der Universität Zürich) for the negative-stain electron microscopy, Andreas Kohl for help with the dynamic light scattering measurements, Michael J. Buchmeier for providing the antibodies WE 18.8 and WE 83.4, Dorothee von Laer for the codon-optimized LCMV-WE GP sequence, Winfried Beyer for the plasmid pHCMV-GP (WE) (AJ318513), and Markus Grütter and Ari Helenius for valuable and helpful discussions.

This work was supported by the Swiss National Science Foundation.

## REFERENCES

1. **Barbouche, R., R. Miquelis, I. M. Jones, and E. Fenouillet.** 2003. Protein-disulfide isomerase-mediated reduction of two disulfide bonds of HIV envelope glycoprotein 120 occurs post-CXCR4 binding and is required for fusion. J. Biol. Chem. **278:**3131–3136.
2. **Beyer, W. R., H. Miletic, W. Ostertag, and D. von Laer.** 2001. Recombinant expression of lymphocytic choriomeningitis virus strain WE glycoproteins: a single amino acid makes the difference. J. Virol. **75:**1061–1064.
3. **Beyer, W. R., D. Popplau, W. Garten, D. von Laer, and O. Lenz.** 2003. Endoproteolytic processing of the lymphocytic choriomeningitis virus glycoprotein by the subtilase SKI-1/S1P. J. Virol. **77:**2866–2872.
4. **Borrow, P., and M. B. Oldstone.** 1992. Characterization of lymphocytic choriomeningitis virus-binding protein(s): a candidate cellular receptor for the virus. J. Virol. **66:**7270–7281.
5. **Bowen, M. D., C. J. Peters, and S. T. Nichol.** 1997. Phylogenetic analysis of the Arenaviridae: patterns of virus evolution and evidence for cospeciation between arenaviruses and their rodent hosts. Mol. Phylogenet. Evol. **8:**301–316.
6. **Bruns, M., L. Martinez Peralta, and F. Lehmann-Grube.** 1983. Lymphocytic choriomeningitis virus. III. Structural proteins of the virion. J. Gen. Virol. **64:**599–611.
7. **Buchmeier, M. J.** 2002. Arenaviruses: protein structure and function, 1st ed., vol. 1. Springer, Berlin, Germany.
8. **Buchmeier, M. J., M. D. Bowen, and C. J. Peters.** 2001. Arenaviridae: the viruses and their replication, 4th ed., vol. 2. Lippincott Williams and Wilkins, Philadelphia, Pa.
9. **Buchmeier, M. J., H. A. Lewicki, O. Tomori, and M. B. Oldstone.** 1981. Monoclonal antibodies to lymphocytic choriomeningitis and pichinde viruses: generation, characterization, and cross-reactivity with other arenaviruses. Virology **113:**73–85.
10. **Buchmeier, M. J., and B. S. Parekh.** 1987. Protein structure and expression among arenaviruses. Curr. Top. Microbiol. Immunol. **133:**41–57.
11. **Buchmeier, M. J., P. J. Southern, B. S. Parekh, M. K. Wooddell, and M. B. Oldstone.** 1987. Site-specific antibodies define a cleavage site conserved among arenavirus GP-C glycoproteins. J. Virol. **61:**982–985.
12. **Burns, J. W., and M. J. Buchmeier.** 1991. Protein-protein interactions in lymphocytic choriomeningitis virus. Virology **183:**620–629.
13. **Calder, L. J., L. Gonzalez-Reyes, B. Garcia-Barreno, S. A. Wharton, J. J. Skehel, D. C. Wiley, and J. A. Melero.** 2000. Electron microscopy of the human respiratory syncytial virus fusion protein and complexes that it forms with monoclonal antibodies. Virology **271:**122–131.
14. **Cao, W., M. D. Henry, P. Borrow, H. Yamada, J. H. Elder, E. V. Ravkov, S. T. Nichol, R. W. Compans, K. P. Campbell, and M. B. Oldstone.** 1998. Identification of alpha-dystroglycan as a receptor for lymphocytic choriomeningitis virus and Lassa fever virus. Science **282:**2079–2081.
15. **Chen, L., P. M. Colman, L. J. Cosgrove, M. C. Lawrence, L. J. Lawrence, P. A. Tulloch, and J. J. Gorman.** 2001. Cloning, expression, and crystallization of the fusion protein of Newcastle disease virus. Virology **290:**290–299.
16. **Ciurea, A., P. Klenerman, L. Hunziker, E. Horvath, B. M. Senn, A. F. Ochsenbein, H. Hengartner, and R. M. Zinkernagel.** 2000. Viral persistence in vivo through selection of neutralizing antibody-escape variants. Proc. Natl. Acad. Sci. USA **97:**2749–2754.
17. **Colman, P. M., and M. C. Lawrence.** 2003. The structural biology of type I viral membrane fusion. Nat. Rev. Mol. Cell Biol. **4:**309–319.
18. **Di Simone, C., and M. J. Buchmeier.** 1995. Kinetics and pH dependence of acid-induced structural changes in the lymphocytic choriomeningitis virus glycoprotein complex. Virology **209:**3–9.
19. **Di Simone, C., M. A. Zandonatti, and M. J. Buchmeier.** 1994. Acidic pH triggers LCMV membrane fusion activity and conformational change in the glycoprotein spike. Virology **198:**455–465.
20. **Durell, S. R., I. Martin, J. M. Ruysschaert, Y. Shai, and R. Blumenthal.** 1997. What studies of fusion peptides tell us about viral envelope glycoprotein-mediated membrane fusion. Mol. Membr. Biol. **14:**97–112.
21. **Dutch, R. E., T. S. Jardetzky, and R. A. Lamb.** 2000. Virus membrane fusion proteins: biological machines that undergo a metamorphosis. Biosci. Rep. **20:**597–612.
22. **Earl, P. L., R. W. Doms, and B. Moss.** 1990. Oligomeric structure of the human immunodeficiency virus type 1 envelope glycoprotein. Proc. Natl. Acad. Sci. USA **87:**648–652.
23. **Earp, L. J., S. E. Delos, H. E. Park, and J. M. White.** 2005. The many mechanisms of viral membrane fusion proteins. Curr. Top. Microbiol. Immunol. **285:**25–66.
24. **Eckert, D. M., and P. S. Kim.** 2001. Mechanisms of viral membrane fusion and its inhibition. Annu. Rev. Biochem. **70:**777–810.
25. **Eichler, R., O. Lenz, T. Strecker, M. Eickmann, H. D. Klenk, and W. Garten.** 2003. Identification of Lassa virus glycoprotein signal peptide as a trans-acting maturation factor. EMBO Rep. **4:**1084–1088.
26. **Froeschke, M., M. Basler, M. Groettrup, and B. Dobberstein.** 2003. Long-lived signal peptide of lymphocytic choriomeningitis virus glycoprotein pGP-C. J. Biol. Chem. **278:**41914–41920.
27. **Gallaher, W. R., C. DiSimone, and M. J. Buchmeier.** 2001. The viral transmembrane superfamily: possible divergence of Arenavirus and Filovirus glycoproteins from a common RNA virus ancestor. BMC Microbiol. **1:**1.
28. **Gallina, A., T. M. Hanley, R. Mandel, M. Trahey, C. C. Broder, G. A. Viglianti, and H. J. Ryser.** 2002. Inhibitors of protein-disulfide isomerase prevent cleavage of disulfide bonds in receptor-bound glycoprotein 120 and prevent HIV-1 entry. J. Biol. Chem. **277:**50579–50588.
29. **Glushakova, S. E., I. S. Lukashevich, and L. A. Baratova.** 1990. Prediction of arenavirus fusion peptides on the basis of computer analysis of envelope protein sequences. FEBS Lett. **269:**145–147.
30. **Glushakova, S. E., V. G. Omelyanenko, I. S. Lukashevitch, A. A. Bogdanov, Jr., A. B. Moshnikova, A. T. Kozytch, and V. P. Torchilin.** 1992. The fusion of artificial lipid membranes induced by the synthetic arenavirus 'fusion peptide'. Biochim. Biophys. Acta **1110:**202–208.
31. **Heinz, F. X., and S. L. Allison.** 2001. The machinery for flavivirus fusion with host cell membranes. Curr. Opin. Microbiol. **4:**450–455.
32. **Imperiali, M., C. Thoma, E. Pavoni, A. Brancaccio, N. Callewaert, and A.**

**Oxenius.** 2005. O mannosylation of alpha-dystroglycan is essential for lymphocytic choriomeningitis virus receptor function. J. Virol. **79:**14297–14308.
33. **Jardetzky, T. S., and R. A. Lamb.** 2004. Virology: a class act. Nature **427:** 307–308.
34. **Jones, D. T.** 1999. Protein secondary structure prediction based on position-specific scoring matrices. J. Mol. Biol. **292:**195–202.
35. **Kielian, M., and F. A. Rey.** 2006. Virus membrane-fusion proteins: more than one way to make a hairpin. Nat. Rev. Microbiol. **4:**67–76.
36. **Kunz, S., J. M. Rojek, M. Kanagawa, C. F. Spiropoulou, R. Barresi, K. P. Campbell, and M. B. A. Oldstone.** 2005. Posttranslational modification of α-dystroglycan, the cellular receptor for arenaviruses, by the glycosyltransferase LARGE is critical for virus binding. J. Virol. **79:**14282–14296.
37. **Kunz, S., N. Sevilla, D. B. McGavern, K. P. Campbell, and M. B. Oldstone.** 2001. Molecular analysis of the interaction of LCMV with its cellular receptor [alpha]-dystroglycan. J. Cell Biol. **155:**301–310.
38. **Lenz, O., J. ter Meulen, H. D. Klenk, N. G. Seidah, and W. Garten.** 2001. The Lassa virus glycoprotein precursor GP-C is proteolytically processed by subtilase SKI-1/S1P. Proc. Natl. Acad. Sci. USA **98:**12701–12705.
39. **Letarov, A. V., Y. Y. Londer, S. P. Boudko, and V. V. Mesyanzhinov.** 1999. The carboxy-terminal domain initiates trimerization of bacteriophage T4 fibritin. Biochemistry (Moscow) **64:**817–823.
40. **Meyer, B. J., J. C. De La Torre, and P. J. Southern.** 2002. Arenaviruses: genomic RNAs, transcription, and replication, 1st ed., vol. 1. Springer, Berlin, Germany.
41. **Neuman, B. W., B. D. Adair, J. W. Burns, R. A. Milligan, M. J. Buchmeier, and M. Yeager.** 2005. Complementarity in the supramolecular design of arenaviruses and retroviruses revealed by electron cryomicroscopy and image analysis. J. Virol. **79:**3822–3830.
42. **Parekh, B. S., and M. J. Buchmeier.** 1986. Proteins of lymphocytic choriomeningitis virus: antigenic topography of the viral glycoproteins. Virology **153:**168–178.
43. **Ruigrok, R. W., A. Aitken, L. J. Calder, S. R. Martin, J. J. Skehel, S. A. Wharton, W. Weis, and D. C. Wiley.** 1988. Studies on the structure of the influenza virus haemagglutinin at the pH of membrane fusion. J. Gen. Virol. **69:**2785–2795.
44. **Ryser, H. J., E. M. Levy, R. Mandel, and G. J. DiSciullo.** 1994. Inhibition of human immunodeficiency virus infection by agents that interfere with thiol-disulfide interchange upon virus-receptor interaction. Proc. Natl. Acad. Sci. USA **91:**4559–4563.
45. **Schawaller, M., G. E. Smith, J. J. Skehel, and D. C. Wiley.** 1989. Studies with crosslinking reagents on the oligomeric structure of the env glycoprotein of HIV. Virology **172:**367–369.
46. **Schibli, D. J., and W. Weissenhorn.** 2004. Class I and class II viral fusion protein structures reveal similar principles in membrane fusion. Mol. Membr. Biol. **21:**361–371.
47. **Seiler, P., U. Kalinke, T. Rulicke, E. M. Bucher, C. Bose, R. M. Zinkernagel, and H. Hengartner.** 1998. Enhanced virus clearance by early inducible lymphocytic choriomeningitis virus-neutralizing antibodies in immunoglobulin-transgenic mice. J. Virol. **72:**2253–2258.
48. **Singh, M., B. Berger, and P. S. Kim.** 1999. LearnCoil-VMF: computational evidence for coiled-coil-like motifs in many viral membrane-fusion proteins. J. Mol. Biol. **290:**1031–1041.
49. **Sissoeff, L., M. Mousli, P. England, and C. Tuffereau.** 2005. Stable trimerization of recombinant rabies virus glycoprotein ectodomain is required for interaction with the p75NTR receptor. J. Gen. Virol. **86:**2543–2552.
50. **Skehel, J. J., and D. C. Wiley.** 2000. Receptor binding and membrane fusion in virus entry: the influenza hemagglutinin. Annu. Rev. Biochem. **69:**531–569.
51. **Spiropoulou, C. F., S. Kunz, P. E. Rollin, K. P. Campbell, and M. B. Oldstone.** 2002. New World arenavirus clade C, but not clade A and B viruses, utilizes α-dystroglycan as its major receptor. J. Virol. **76:**5140–5146.
52. **Stevens, J., A. L. Corper, C. F. Basler, J. K. Taubenberger, P. Palese, and I. A. Wilson.** 2004. Structure of the uncleaved human H1 hemagglutinin from the extinct 1918 influenza virus. Science **303:**1866–1870.
53. **Wallin, M., M. Ekstrom, and H. Garoff.** 2004. Isomerization of the intersubunit disulphide-bond in Env controls retrovirus fusion. EMBO J. **23:**54–65.
54. **Weber, E. L., and M. J. Buchmeier.** 1988. Fine mapping of a peptide sequence containing an antigenic site conserved among arenaviruses. Virology **164:**30–38.
55. **Wright, K. E., R. C. Spiro, J. W. Burns, and M. J. Buchmeier.** 1990. Post-translational processing of the glycoproteins of lymphocytic choriomeningitis virus. Virology **177:**175–183.
56. **Yang, X., J. Lee, E. M. Mahony, P. D. Kwong, R. Wyatt, and J. Sodroski.** 2002. Highly stable trimers formed by human immunodeficiency virus type 1 envelope glycoproteins fused with the trimeric motif of T4 bacteriophage fibritin. J. Virol. **76:**4634–4642.